

## Research Article

# Quantitative Characterization of Agglomerate Abrasion in a Tumbling Blender by Using the Stokes Number Approach

Tofan A. Willemsz,<sup>1,2,5</sup> Tien Thanh Nguyen,<sup>1,2</sup> Ricardo Hooijmaijers,<sup>2</sup> Henderik W. Frijlink,<sup>1</sup> Herman Vromans,<sup>3</sup> and Kees van der Voort Maarschalk<sup>1,4</sup>

Received 30 July 2012; accepted 7 December 2012; published online 19 December 2012

**Abstract.** Removal of microcrystalline cellulose agglomerates in a dry-mixing system (lactose, 100 M) predominantly occurs *via* abrasion. The agglomerate abrasion rate potential is estimated by the Stokes abrasion ( $St_{Abr}$ ) number of the system. The  $St_{Abr}$  number equals the ratio between the kinetic energy density of the moving powder bed and the work of fracture of the agglomerate. Basically, the  $St_{Abr}$  number concept describes the blending condition of the dry-mixing system. The concept has been applied to investigate the relevance of process parameters on agglomerate abrasion in tumbling blenders. Here, process parameters such as blender rotational speed and relative fill volumes were investigated. In this study, the  $St_{Abr}$  approach revealed a transition point between abrasion rate behaviors. Below this transition point, a blending condition exists where agglomerate abrasion is dominated by the kinetic energy density of the powder blend. Above this transition point, a blending condition exists where agglomerates show (undesirable) slow abrasion rates. In this situation, the blending condition is mainly determined by the high fill volume of the filler.

**KEY WORDS:** agglomerates; dry-mixing; stokes; tumbling blender.

## INTRODUCTION

The tumbling blender is currently one of the most common mixers used in the pharmaceutical industry. The device has received considerable attention both in theoretical and practical approaches that describe the mechanisms of particle motion in these blenders and resulting mixing performance (1–4). Obtaining the correct blending conditions is crucial because this safeguards formation of sufficiently uniform blends (5,6). In practice, a blend mostly contains different powders with both cohesive and free-flowing properties. An often encountered system is a cohesive powder that needs to be blended into free-flowing bulk powder. Cohesive powders tend to form agglomerates (7). Removal of these agglomerates and prevention of the formation of new agglomerates are often critical in the assessment of the uniform blend. It is essential that the blender is capable of removing the

agglomerates. In such situations, the rate of agglomerate removal determines the required blending time. In practice, blending conditions are not always capable of removing agglomerates sufficiently fast leading to undesired excessively long mixing times or to blend inhomogeneity.

Removal of agglomerates in a dry-mixing system predominantly occurs *via* abrasion (7,8). It appeared to be possible to explain the agglomerate abrasion process in convection blender by definition of the Stokes abrasion number ( $St_{Abr}$ ). This number is the ratio of the kinetic energy density of the powder bed to the work of fracture of the agglomerate and describes the blending condition of the dry-mixing system (9).

Currently, only limited studies have been reported on the influence of blending conditions on agglomerate abrasion in tumbling blenders. The aim of this study was to investigate the relevance of process parameters that describe the blending conditions on agglomerate abrasion in tumbling blenders.

## EXPERIMENTAL

### Materials

The materials used were microcrystalline cellulose (MCC) (Avicel PH-101, FMC, Philadelphia, USA) and  $\alpha$ -lactose monohydrate (Pharmatose® 100 M from DMV Fontterra Excipients, Goch, Germany, with a bulk density of 750 kg/m<sup>3</sup>), which acted as filler.

<sup>1</sup>Department of Pharmaceutical Technology and Biopharmacy, University of Groningen, A. Deusinglaan 1, 9713 AV Groningen, The Netherlands.

<sup>2</sup>Pharmaceutical Sciences and Clinical Supplies, Merck MSD, PO Box 20, 5340 BH Oss, The Netherlands.

<sup>3</sup>Department of Pharmaceutics, Utrecht Institute for Pharmaceutical Sciences (UIPS), Utrecht University, PO Box 80082, 3508 TB Utrecht, The Netherlands.

<sup>4</sup>Competence Center Process Technology, Purac Biochem, PO Box 214200 AA Gorinchem, The Netherlands.

<sup>5</sup>To whom correspondence should be addressed. (e-mail: tofan.willemsz@merck.com)

## Methods

### Model Agglomerates (Brittle Calibrated Test Particles)

The model agglomerates or spherical brittle calibrated test particles (bCTPs) were prepared from MCC as described before by Willemsz *et al.* (8). The porosities of all bCTPs produced were measured from the diameters and the weights of the bCTPs. The true density of the MCC was determined using a pycnometer (AccuPyc 1330, Micromeritics, Norcross, USA) using nitrogen as test gas and was found to be (1,600 kg/m<sup>3</sup>). The mechanical properties (Young's modulus,  $Y$ , and strength,  $\sigma_s$ ) of the bCTPs were characterized as described in Willemsz *et al.* (10).

### Blending Tests

The blending experiments reported in this study were performed using a tumbling blender with bowl volume of 10 L (Bohle model LM40, Germany, unbaffled). Loaded with the filler and bCTPs, the relative fill volume ( $\varphi$ ) varied between 40% and 80% (V/V). A test was started by adding selected test particles to the filler. This mixture was placed in the blender and rotated at rates between 20, 30, and 40 RPM. After a given blending time, the blend was sieved over a 500- $\mu$ m sieve to collect the test particles. The weights and dimensions of the bCTPs were determined as a function of blending time. These values were used to calculate the abrasion rate according to Eq. 1. Details of the experiment are mentioned in the previous publication (8).

### Powder Surface Velocimetry

To collect data from powder surface velocimetry, a Plexiglas lid was placed on the blender. The camera was mounted on top of the blender perpendicular to the Plexiglas lid and such that about 70% of the total powder surface was visible. The powder surface velocimetry data were collected by recording through the watch glass of the apparatus. The powder flow was recorded using a high-speed video camera (Casio-EX-F1, Casio Computer Co., Ltd, Tokyo, Japan) operating at a speed of 600 frames per second. The data were analyzed according to Willemsz *et al.* [10] to gain powder surface velocities.

The position of the camera changes relative to the powder surface as an effect of the rotation of the blender. This is schematically depicted in Fig. 1. The angle of observation of the camera relative to the surface of the bed is needed to calculate the surface velocity from the images.

This angle is simply determined from the mean dynamic angle of repose of lactose 100 M, of which the average value is reported to be 60.3° (11,12), and the angle of the camera with the horizontal plane. The dynamic angle of repose was assumed to be independent from the blender rotational rates used in this study (11,12).

### DEM Simulations

To clarify the experimental results, a simulation of the movements of 10,000 particles in a container mixer was carried out using the discrete element method (DEM) (13). Each

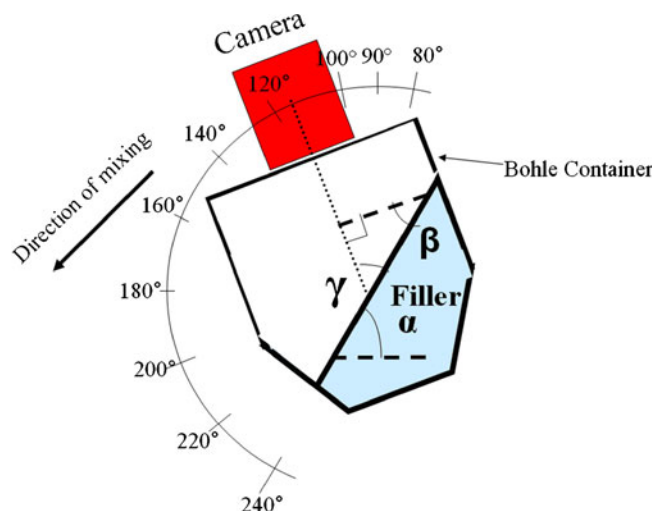


**Fig. 1.** Camera position relative to the powder bed (with  $\alpha$  as the dynamic angle of repose of the powder bed,  $\beta$  the angle observation of the camera, and  $\gamma$  the angle observation of the camera relative to the powder bed)

particle in the simulation was created by overlapping three spheres of 100  $\mu$ m in diameter to make a rod-like particle with dimensions of 100 $\times$ 200  $\mu$ m. The particle's density is 1,500 kg/m<sup>3</sup> which is similar to that of lactose. The container size and dimensions are shown in Fig. 2. The volume of the container is 2 $\times$ 10<sup>-4</sup>L corresponding to a fill level of approximately 40% (V/V). The container mixer was rotated at a speed of 120 rpm. The Hertz-Mindlin contact model was used for particle-to-particle interaction and particle-to-geometry interaction (14). The simulation was done using the EDEM 2.4.1 package (DEM Solutions, UK).

### Statistical Analyses

Standard deviation (SD) and 95% confidence interval calculations described in this paper were performed using SAS V9.1 software (SAS institute Inc., North Carolina, USA).

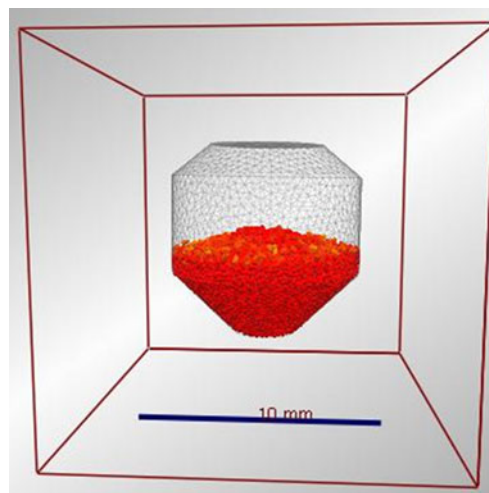


**Fig. 2.** Size and dimensions of the container mixer used in DEM simulation

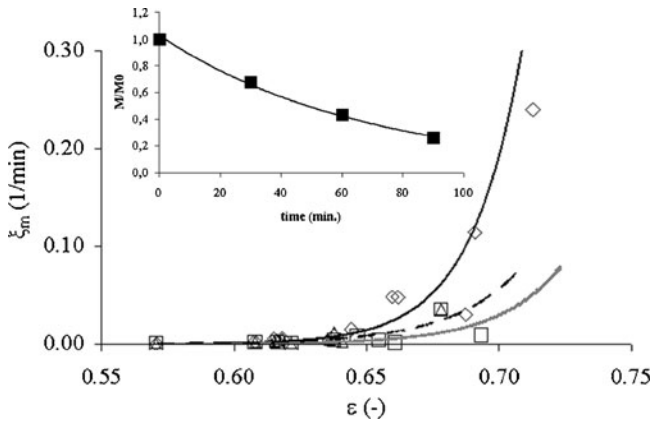


**Fig. 3.** The effect of the mass-based abrasion rate constant at a blender rotational rate ( $\omega$ ) of 20 RPM (white squares), 30 RPM (white triangles), and 40 RPM (white diamonds) and a constant relative fill volume of 40% (V/V). The *inner graph* shows a typical example of  $M_{rel}$  over time

## RESULTS AND DISCUSSION

### Abrasion Rate Constant ( $\xi_m$ ) Measurements in the Tumbling Blender

In this study, a tumbling mixer was used to assess how the abrasion rate constants ( $\xi_m$ ) (8) of brittle agglomerates are affected by process variables in the tumbling blender. The bCTP's mass reduction ( $M_{rel}$ ) over time was determined and appeared to obey apparent first-order kinetics as demonstrated in our previous work (8). A typical example is shown in the inset of Fig. 3.

$$M_{rel} = \frac{M(t)}{M_0} = e^{-\xi_m * t} \quad (1)$$

with  $M(t)$  as the mass after blending time  $t$  and  $M_0$ , the initial mass.

Figure 3 shows the effect of blender rotational rate ( $\omega$ ) on the abrasion rate constants of agglomerates with different porosities. Figure 3 shows that the abrasion rate constants of the agglomerates increase with blender rotational rate. These findings are in line with findings discussed in previous papers: Loveday and Naidoo (15) showed that rock abrasion increases with mill speed in autogenous milling. Khanal and Morrison (16) demonstrated that the abrasion of particles increases with the rotational speed of the mill in a small scale tumbling mill

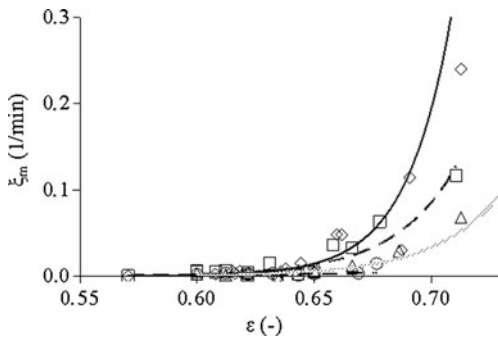


**Fig. 4.** The effect of the mass-based abrasion rate constant at a relative fill volume of 40% (V/V) (white diamonds) (solid line), 53% (V/V) (white squares) (dashed line), 67% (V/V) (white triangles) (gray dotted line), and 80% (V/V) (white circles) (dotted line) and a constant container rotational rate of 40 RPM

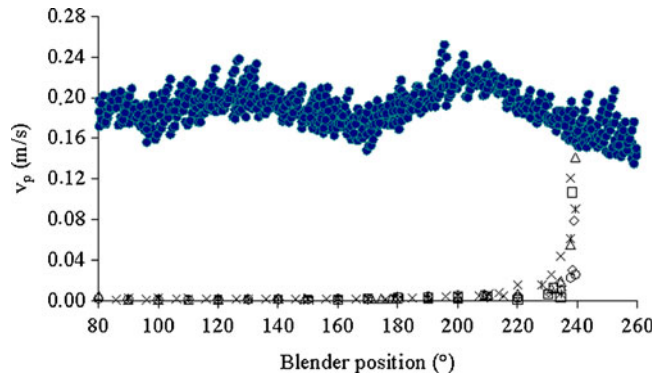


**Fig. 5.** Powder surface velocities observed by the camera ( $v_p$ ) at different fill volumes ( $\phi$ ) and container rotational speeds ( $\omega$ ) (experimental: white diamonds:  $\phi=40\%$  (V/V),  $\omega=20$  RPM; white squares:  $\phi=40\%$  (V/V),  $\omega=30$  RPM; white triangles:  $\phi=40\%$  (V/V),  $\omega=40$  RPM; X marks:  $\phi=53\%$  (V/V),  $\omega=40$  RPM; asterisks:  $\phi=67\%$  (V/V),  $\omega=40$  RPM; white circles:  $\phi=80\%$  (V/V),  $\omega=40$  RPM). Velocity of cascading layer obtained by DEM calculations: black circles:  $\phi=40\%$  (V/V),  $\omega=40$  RPM

environment. Finally, Willemsz *et al.* (8) showed that agglomerate abrasion increases with impeller rotational speed in convective blenders.

Relative fill volume is known to have a significant impact on mixing efficiency (6). Relative fill volume has also been identified as a critical parameter that affects agglomerate abrasion during dry-mixing processes in convection mixers (1,2). For this reason, relative fill volumes were varied to assess how the abrasion rate constants of agglomerates depend on relative fill volumes in tumbling mixers. The results are given in Fig. 4.

Figure 4 shows that the abrasion rate constants have lower values at a given aggregate porosity when fill degree increases. The figure also shows that the abrasion rates of agglomerates at a (high) relative fill volume of 80% (V/V) do not seem to have a strong and logical correlation with aggregate porosity.

A visual assessment of the powder bed revealed that the model agglomerates (bCTPs) emerge frequently on the surface of the powder bed. This is not surprising because the density of the agglomerates is low. The surface of the powder bed in diffusion blenders such as the one used in this study has been described before (3,17,18). They indicated the presence of a thin powder layer flowing at high velocity, called the cascading layer. A slower-moving region exists below the cascading layer (3,17). It was shown that all mixing takes place in the cascading region. Below this region, the powder mixture behaves much like a solid body rotating along with the tumbler. Virtually no powder mixing takes place in this region since individual particles are not in

**Table I.** Powder Surface Velocity ( $v_p$ ) at Various Container Rotational Speeds ( $\omega$ ) and Fill Volumes ( $\phi$ )

$\phi$ (%)	$\omega$ (RPM)	$v_p \pm SD$ (m/s)
40	20	0.079 $\pm$ 0.017
	30	0.107 $\pm$ 0.015
	40	0.141 $\pm$ 0.016
53	40	0.121 $\pm$ 0.024
67	40	0.090 $\pm$ 0.019
80	40	0.026 $\pm$ 0.012

RPM revolutions per minute, SD standard deviation

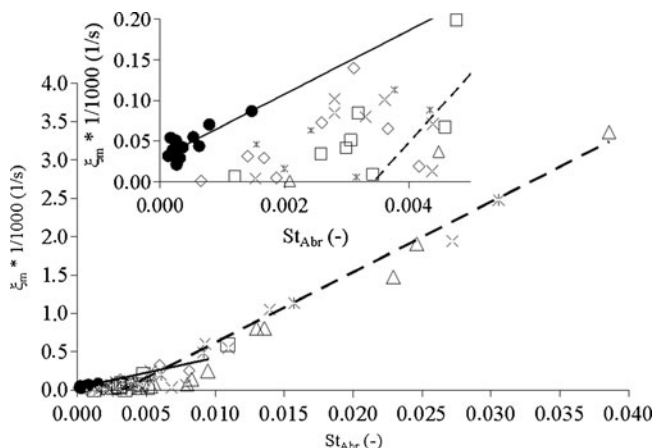


**Fig. 6.** The relationship between the abrasion rate constants and the Stokes abrasion number of various bCTPs at  $\phi=40\%$  ( $V/V$ ),  $\omega=20$  RPM (white diamonds);  $\phi=40\%$  ( $V/V$ ),  $\omega=30$  RPM (white squares);  $\phi=40\%$  ( $V/V$ ),  $\omega=40$  RPM (white triangles);  $\phi=53\%$  ( $V/V$ ),  $\omega=40$  RPM (X marks);  $\phi=67\%$  ( $V/V$ ),  $\omega=40$  RPM (asterisks); and  $\phi=80\%$  ( $V/V$ ),  $\omega=40$  RPM (black circles). The inner graph shows an enlarged region of the region of low  $St_{Abr}$  values

motion relative to each other (3). Blending conditions affect the powder velocity of the cascading layer (3,4,18).

Our previous work showed that filler powder velocity is an important parameter in relation to the abrasion rate constant of agglomerates (8,19). For this reason, the following step is to evaluate effects of the speed of the cascading layer on the abrasion rate constants of agglomerates.

#### Powder Surface Velocity and Stokes abrasion number ( $St_{Abr}$ )

The powder velocities were determined at various blender positions as described in the “Materials” and “Methods” sections. Figure 5 shows the blender positions and corresponding particle velocities in the cascading layer at different tumbling rates and relative fill degrees. When the position of the blender exceeds  $240^\circ$ , the powder bed covers the watch glass. As a result, the camera does not detect any powder movement. This part of the powder bed hardly moves. At a certain moment in the rotation, the powder obtains the freedom to move, and a sharp increase in particle velocity is recorded. This is the movement of the cascading layer of the bed, and the camera actually observes the moving particles.

According to Sudah *et al.* (3) and Lumieux *et al.* (18), the particle velocity is moderately dependent on the blender position (*e.g.*). This is confirmed by DEM simulation data as shown in Fig. 5. The DEM data show that the particle

velocities in the cascading layer are moderately dependent on blender position. The particle velocity that has been estimated using DEM is in line with the maximum velocity experimentally observed. For this reason, the experimentally determined particle velocity has been detected under different conditions. Table I reports the results of particle velocity at various container rotational speeds ( $\omega$ ) and fill volumes ( $\phi$ ). A clear effect of container rotational speed and fill volume ( $\phi$ ) on particle velocity is visible.

Table I shows that  $v_p$  increases with increasing container rotational rates but decreases with increasing fill volumes. Figures 3 and 4 show the effects of container rotational rates and relative fill volume on the abrasion rate constants of the agglomerates. These effects are correlated using the Stokes abrasion number ( $St_{Abr}$ ). The Stokes abrasion number concept has been discussed earlier in more detail in previous papers (9,19):

$$St_{abr} = \frac{\rho_b \cdot v_p^2 \cdot Y}{\sigma_c^2} \quad (2)$$

with  $\rho_b$  as bulk density of the filler. The mechanical properties of the bCTPs (Young’s modulus,  $Y$ , and strength,  $\sigma_s$ ) have been measured as previously described (9) and are based on the porosity values of the agglomerates.

Figure 6 shows the relationship between the abrasion rates and the Stokes abrasion numbers in the blending experiments at different working conditions. Figure 6 shows two more or less distinct groups of data: (1) one with the largest group of tests at fill levels below  $67\%$  ( $V/V$ ) with rotational rates of 30 and 40 RPM which is valid at a relatively high Stokes number range and (2) a much more scattered data set at a fill level of  $80\%$  ( $V/V$ ) which shows faster abrasion at low Stokes numbers.

Model diagnostic plots of the data set show that both variables ( $\xi_m$  and  $St_{Abr}$ ) should be log transformed before analysis to fulfill the statistical requirements for normal distribution of the values. The two relationships depicted in Fig. 6 were analyzed accordingly. The statistical analysis leads to a regression model for both relationships:

$$\text{Log}(\xi_m) = \beta + \alpha_i \times \text{log}(St_{Abr}) \quad (3)$$

Table II lists the models produced.

The  $R^2$  in Table II shows that the  $St_{Abr}$  number is a reasonable way to predict agglomerate abrasion during a diffusive blending process when the  $\phi$  is lower than  $67\%$  ( $V/V$ ) because the proposed model explains  $77\%$  of agglomerate

**Table II.** The Regression Models Between  $\xi_m$  and  $St_{Abr}$  for the Curves Depicted in Fig. 6

Process condition	$\omega$ (RPM)	Variable	Estimate	95% Confidence limits		$R^2$ (%)
				Lower	Upper	
$\phi < 67\%$ ( $V/V$ ) (dashed line in Fig. 6)	20–40	$\beta$	3.27	2.95	3.60	77
		$\alpha_i$	1.88	1.74	2.01	
$\phi = 80\%$ ( $V/V$ ) (solid line in Fig. 6)	40	$\beta$	−0.11	0.03	−0.26	41
		$\alpha_i$	0.36	−0.13	0.85	

RPM revolutions per minute



abrasion. In this situation, agglomerate abrasion is affected by the parameters that calculate the  $St_{Abr}$  number of the system. It is noted, however, that the quality of prediction is lower when compared to convective mixers (9). In contrast, when  $\phi$  is 80% (V/V) the proposed model explains only 41% of agglomerate abrasion. This implies that in this situation, agglomerate abrasion is basically driven by a different mechanism.

According to Fig. 4, a high fill level leads to slower abrasion of the test particles. Moreover, particle velocity in the cascading layer is low (Fig. 5 and Table I) implicating that the proposed model insufficiently explains agglomerate abrasion. A high fill level has less tumbling space available (so lower circulation per revolution) compared to lower fill volumes. This reduces the effect of the cascading layer (3,17). To assess the validity of the model, more separate regression analyses have been performed for all relative fill volumes and rotational rates. Figure 7 summarizes these results.

Figure 7 shows that both the fit parameters  $\alpha$  and  $\beta$  and the coefficient of regression ( $R^2$ ) are high when fill volumes are low. The values of the parameters in Fig. 7 illustrate that  $\alpha$ ,  $\beta$ , and  $R^2$  are almost independent of the relative fill volume when this is below 67% (V/V). This implicates that the relationships between abrasion rate and  $St_{Abr}$  almost overlap, *i.e.*, the relation between abrasion rate constant and Stokes number is highly independent of the relative fill volumes. This is confirmed by the very small change in each parameter plotted in Fig. 7 below 70% (V/V). A fill volume of 80% (V/V) shows a totally different behavior (Figs. 6 and 7). The impact of the cascading layer decreases significantly when fill degree is above approximately 70% (V/V).

From a practical standpoint, this blending condition is not desired due to the (extremely) slow abrasion rates and therefore deficient potential to remove agglomerates. The removal of agglomerates and prevention of the formation of new agglomerates are often the critical steps in the assessment of

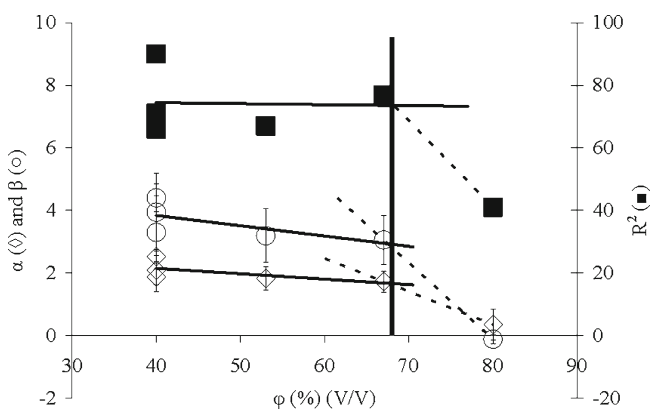


**Fig. 7.** Relationships between the slopes ( $\alpha_i$ , white diamonds) and intercepts ( $\beta$ , white circles) according to Eq. 3 with relative fill volumes ( $\phi$ ) in the tumbling blender and their corresponding  $R^2$  (black squares) values. The solid vertical line indicates the transition point between a blending condition where agglomerate abrasion is dominated by the kinetic energy density of the powder blend and a blending condition where agglomerate abrasion rate is extremely low. Error bars at  $\alpha_i$  and  $\beta$  indicate the  $\pm 95\%$  confidence limits

the uniform blend (7,8). This means that obtaining the correct blend conditions is crucial because only this safeguards the formation of a sufficiently uniform blend.

## CONCLUSION

The abrasion of agglomerates during dry-mixing at different blending conditions has been investigated in a tumbling blender. For this investigation, the  $St_{Abr}$  number concept has been applied and revealed a transition point. Below this transition point, a blending condition exists where agglomerate abrasion is dominated by the kinetic energy density of the powder blend. Above this transition point, a blending condition exists where agglomerates show (undesirable) slow abrasion rates. In this situation, the blending condition is mainly determined by the high fill volume of the filler.

## ACKNOWLEDGMENTS

This study was performed within the framework of Top Institute Pharma project number D6-203.

## REFERENCES

1. Sudah OS, Coffin-Beach D, Muzzio FJ. Effects of blender rotational speed and discharge on the homogeneity of cohesive and free flowing mixtures. *Int J Pharm.* 2002;247:57–68.
2. Sudah OS, Coffin-Beach D, Muzzio FJ. Quantitative characterization of mixing of free-flowing granular material in tote (bin)-blenders. *Powder Technol.* 2002;126:191–200.
3. Sudah OS, Arratia PE, Alexander A, Muzzio FJ. Simulation and experiments of mixing and segregation in a tote blender. *AIChE J.* 2005;51–3:836–44.
4. Arratia PE, Duong N, Muzzio FJ, Godbole P, Reynolds S. A study of the mixing and segregation mechanisms in the Bohle tote blender via DEM simulations. *Powder Technol.* 2006;164:50–7.
5. Muzzio FJ, Shinbrot T, Glasser BJ. Powder technology in the pharmaceutical industry: the need to catch up fast. *Powder Technol.* 2002;124:1–7.
6. Muzzio FJ, Alexander AW. Scale-up of powder-blending operations. *Pharm. Technol.* 2005. Mar 1.
7. Kuwagi K, Horio M. A numerical study on agglomerate formation in a fluidized bed of fine cohesive particles. *Chem Eng Sci.* 2002;57:4737–44 (8).
8. Willemsz TA, Oostra W, Hooijmaijers R, De Vegt O, Morad N, Vromans H, Frijlink HW, Van der Voort Maarschalk K. Blending of agglomerates into powders 1: quantification of abrasion rate. *Int J Pharm.* 2010;387(1–2):87–92.
9. Willemsz TA, Hooijmaijers RAA, Rubingh CM, Tran TN, Frijlink HW, Vromans H, Van der Voort Maarschalk K. Kinetic energy density and agglomerate abrasion rate during blending of agglomerates into powders. *Eur J Pharm Sci.* 2012;45:211–5.
10. Willemsz TA, Tran TN, van der Hoeven M, Hooijmaijers RAA, Frijlink HW, Vromans H, Van der Voort Maarschalk K. A statistical method for velocity detection in moving powder beds using image analysis. *AIChE J.* 2011;58(3):690–6.
11. Munoz-Ruiz A, *et al.* Rheology and compression characteristics of lactose based direct compression excipients. *Int J Pharm.* 1993;95:201–7.
12. Bodhmag A. Correlation between physical properties and flowability indicators for fine powders. Thesis. Department of Chemical Engineering University of Saskatchewan Saskatoon, Saskatchewan; 2006. 88.
13. Cundall PA, Strack ODL. Discrete numerical model for granular assemblies. *Geotechnique.* 1979;29(1):47–65.

14. DEMSolutions. Theory reference guide. 2011. <http://www.dem-solutions.com/>. Accessed 14 Dec 2012.
15. Loveday BK, Naidoo D. Rock abrasion in autogeneous milling. *Miner Eng.* 1997;10:603–12.
16. Khanal M, Morrison R. Discrete element method study of abrasion. *Miner. Eng* 2008;21:751–60.
17. Jaeger HM, Nagel SR. Physics of the granular state. *Science.* 1992;255:1523–31.
18. Lemieux M, Bertrand F, Chaoukia J, Gosselin P. Comparative study of the mixing of free-flowing particles in a V-blender and a bin-blender. *Chem Eng Sci.* 2007;62:1783–802.
19. Willemsz TA, Hooijmaijers R, Rubingh CM, Frijlink HW, Vromans H, Van der Voort Maarschalk K. The stokes number approach to support scale-up and technology transfer of a mixing process. *AAPS PharmSciTech.* 2012. doi:10.1208/s12249-012-9818-z.